

A novel dynamic boundary model of pressure propagation for volume fractured horizontal wells in shale oil reservoirs with developed natural fractures

Binyu Wang¹, Linsong Cheng^{1*}, Yafei Zhang¹, Renyi Cao¹

1 China University of Petroleum-Beijing 18, Fuxue Road, Changping District, Beijing, China 102249

(*Corresponding Author: Linsong Cheng Email: lscheng@cup.edu.cn)

ABSTRACT

With the international energy demand and the development of exploration and development technology, the development of shale reservoirs has gradually become a hot topic all over the world, and the existing theories of fluid flow can no longer accurately characterize and describe the flow characteristics of shale oil reservoirs. The formation pressure performances in shale reservoirs are quite different with that of conventional reservoirs due to the strong low-velocity nonlinear flow and starting pressure gradients, which will result in dynamic boundary. Few research mentioned the effects of dynamic boundary caused by the flow mechanism in shale oil reservoirs. In this paper, the nonlinear equation of shale oil reservoirs, segmented linearization, division of the flow space into matrix and SRV regions, application of the source function and Newman product method, and creation of finite-length strip source functions are employed to analyze the effects of dynamic boundary. A novel model of unsteady flow in horizontal wells with multi-fractured section volume fracturing taking the development of natural fractures into consideration was established, and the method of solving the pressure of this model by applying the iterative method of immovable point was put forth using the principles of pressure superposition and unsteady flow superposition. The characteristics of the dynamic boundary of pressure propagation in volume fractured horizontal wells were determined, as well as the effects of various reservoir physical parameters on the movement of the dynamic boundary, with the aid of the proposed mathematical model of unsteady flow in volume fractured horizontal wells taking the development of natural fractures into consideration. The analysis demonstrates that, under the nonlinear flow condition, the formation pressure propagation manifests as a dynamic boundary problem. The pressure

propagation dynamic boundary expands more quickly in the early period due to the natural fractures in the reservoir, but tends to stabilize in the later period, indicating the existence of a limiting distance for pressure mobilization in the reservoir. The major determinants of formation pressure wave and mobilization are the physical characteristics of the reservoir (permeability, natural fractures). The stronger the flow nonlinearity and the more developed the natural fractures, the greater the degree of effects on pressure propagation.

Keywords: Natural fractures, Shale oil reservoirs, Dynamic boundary, Nonlinear flow

NONMENCLATURE

Abbreviations

SRV Stimulated Rock Volumes

Symbols

| | |
|----------|--|
| v | Flow rate, m/s |
| p | Transient pressure, MPa |
| p_e | Initial pressure, MPa |
| p_m | Matrix pressure, MPa |
| p_f | Natural fracture pressure, MPa |
| p_{wf} | Bottom hole pressure, MPa |
| r | Displacement radius, m |
| K | Permeability, mD |
| K_m | Matrix permeability, mD |
| K_f | Natural fracture permeability, mD |
| μ | Viscosity, mPa·s |
| G_a | Critical threshold pressure gradient, MPa/m |
| G_b | Intended threshold pressure gradient, MPa/m |
| η_t | Transient pressure conductivity, m ² /s |

| | |
|------------|--|
| t | Time, s |
| τ | Ephemeral moment, s |
| r_w | Wellbore radius, m |
| Q | Production, m ³ /s |
| B | Volume factor, dimensionless |
| H | Thickness of formation, m |
| $R(t)$ | Dynamic boundary, m |
| δV | Ephemeral source, m ³ |
| ϕ | Porosity, dimensionless |
| ϕ_m | Matrix porosity, dimensionless |
| ϕ_f | Natural fracture porosity, dimensionless |
| C | Total compression factor, MPa ⁻¹ |
| x_w | X-coordinate of source, m |
| y_w | Y-coordinate of source, m |
| x_f | Width of strip source, m |
| x_e | Distance of the outer boundary in the x-direction of the SRV region, m |
| y_e | Distance of the outer boundary in the y-direction of the SRV region, m |
| δ | Dirac function |

1. INTRODUCTION

With the rapid development of the global economy, the demand for energy is getting bigger and bigger, the exploitation of conventional oil and gas reservoirs can no longer meet the needs of development, and there is an urgent need to develop new strategic replacement areas for oil resources. Among the unconventional resources, shale reservoirs have huge potential and wide distribution, so the efficient development of shale reservoirs is one of the hot research interests to solve the problem of energy demand and ease pressure on energy supply. Shale oil reservoirs are common examples of integrated source-reservoir petroleum accumulations with extensively developed nanoscale and microscale pore throats, some of which form naturally [1]. The structure of the world's energy supply has changed as a result of shale oil and gas development and the advancement of hydraulic fracturing technology [2]. The actualization of industrial oil flow in shale reservoirs is followed by a number of issues, including low natural production capacity of wells in the field's actual production, quickly declining production, and constrained well use. According to studies, shale oil reservoirs have pore distribution and pore-throat connectivity that are very different from conventional reservoirs. As a result, fluid flow of shale oil exhibits low-velocity nonlinear flow and initiates a pressure gradient,

which has an impact on how effectively the reservoir is used throughout the development process [3–4].

Several semi-analytical and numerical models have been proposed to evaluate the dynamic properties of flow in reservoirs. By using the grid finite difference method, Yu [5] developed the nonlinear flow mathematical model to forecast the dynamic properties of reservoir flow and proposed the permeability loss coefficient to represent the dynamic change of permeability during reservoir development. To create a mathematical model of three-phase fluids' nonlinear flow that could be solved using numerical techniques, Xu [6] developed a novel nonlinear flow model. In order to extract the expected pressure profiles for each time step outside the boundary of the reference equation, Bezyan Yashar [7] discretized the second order nonlinear partial differential equation based on the law of conservation of mass and newly applied particle swarm optimization as a nonlinear solver. Researchers like Jia, Cao, and Wang [8–10] have also studied nonlinear flow features.

Although several models have been proposed, the majority of these studies do not take into account mathematical models that naturally fracture. In order to solve the model's pressure, this paper divides the formation into matrix and SRV regions, creates an unsteady semi-analytical model for volume fractured horizontal wells with multiple fracture segments, takes into account the development of natural fractures, and iteratively solves the model's pressure.

2. PHYSICAL MODEL AND ASSUMPTIONS

The mathematical model of volume fractured horizontal wells has now been rationalized with simplifications and assumptions in order to increase the speed and accuracy of the model calculation. These assumptions are as follows:

(1) Ignoring the impact of boundary circumstances, the fracture segments entirely traverse the production formation, which is a homogenous, equal-thickness infinity formation.

(2) Single-phase flow in the matrix and reservoir fractures.

(3) Ignore the fluid's compressibility, the effect of capillary forces on the fluid flow, or gravity, the flow process is unsteady flow under isothermal conditions.

(4) By using a modified nonlinear flow equation of motion, the fluid flow law—which deviates from Darcy's flow law—is described.

After volume fracturing, the SRV region is consisted of hydraulic fractures and natural fractures. The complex fracture network and reforming segments can be

simplified for the study of the macro-pressure wave and law of the formation, and the SRV region is simplified into a homogenous rectangular fracture network region as shown in Fig. 1.

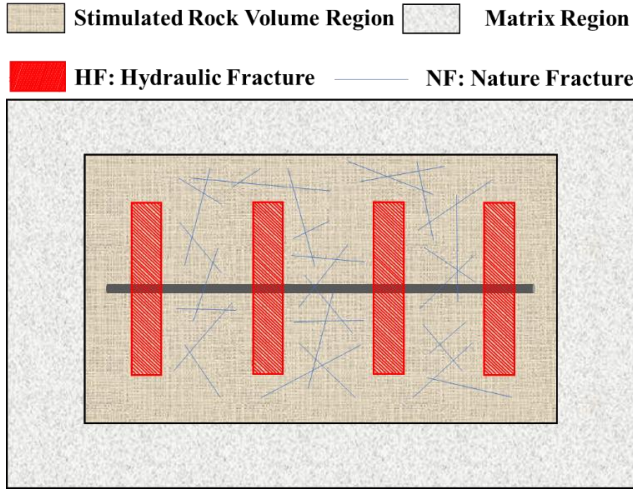


Fig. 1 Schematic of volume fractured horizontal well considering developed natural fractures

3. MATHEMATICAL MODEL AND SOLUTION

The mathematical model of volume fractured horizontal wells has now been rationalized with

3.1 Flow source function construction

The fluid flow at each transient time can be thought of as linear by linearizing the nonlinear equations of flow, and by applying the source function, a mathematical model can be created. A strip source of infinite length is created by organizing an infinite number of line sources in an endless plane. Assume that dl , or the transient flow rate of the source per unit width of the strip, equals ds/dx , or the transient flow rate of the line source per unit length. Integrate the line source function at $x_w \in (x_w - x_f/2, x_w + x_f/2)$. Define the strip source center as x_w and the width as x_f . It is known that the line source function [11] has the following form:

$$\frac{\phi c}{\delta} [p_c - p(x, t)] = \frac{\exp\left[-\frac{(x - x_w)^2}{4\eta t}\right]}{\sqrt{4\pi\eta t}} \quad (1)$$

Get:

$$p(x, t) = p_c - \frac{dl}{\phi c \sqrt{4\pi\eta(t - \tau)}} \int_{x_w - x_f/2}^{x_w + x_f/2} \exp\left[-\frac{(x - x_w)^2}{4\eta(t - \tau)}\right] dx_w \quad (2)$$

Also define the error function as:

$$\text{erf}(x) = \frac{2}{\sqrt{\pi}} \int_0^x \exp(-u^2) du \quad (3)$$

Integrating and simplifying the equation (1), the strip source function is obtained in the form:

$$\frac{\phi c}{\delta} [p_c - p(x, t)] = \frac{1}{2} \left[\text{erf} \frac{\frac{x_f}{2} + (x - x_w)}{\sqrt{4\eta t}} + \text{erf} \frac{\frac{x_f}{2} - (x - x_w)}{\sqrt{4\eta t}} \right] \quad (4)$$

3.2 Mathematical modeling of nonlinear transient pressure considering natural fractures

Suppose there are two sources of infinitely long strips in different directions of the plane, as shown in Fig. 2. The center of the strip source in the vertical X-axis direction is x_w and the width is x_f , and the center of the strip source in the parallel X-axis direction is y_w and the width is y_f . The expression for the source function of the strips in different directions is:

$$S(x, t) = \frac{1}{2} \left[\text{erf} \frac{\frac{x_f}{2} + (x - x_w)}{\sqrt{4\eta t}} + \text{erf} \frac{\frac{x_f}{2} - (x - x_w)}{\sqrt{4\eta t}} \right] \quad (5)$$

$$S(y, t) = \frac{1}{2} \left[\text{erf} \frac{\frac{y_f}{2} + (y - y_w)}{\sqrt{4\eta t}} + \text{erf} \frac{\frac{y_f}{2} - (y - y_w)}{\sqrt{4\eta t}} \right] \quad (6)$$

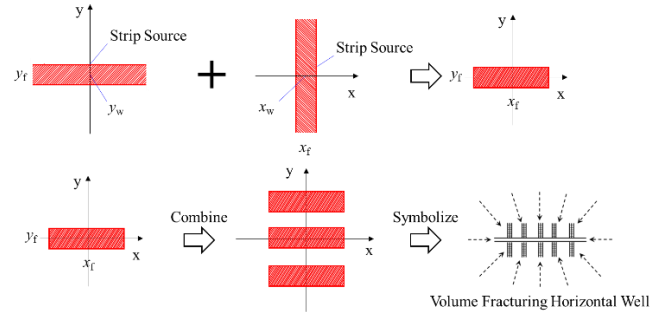


Fig. 2 Schematic of the model coordinate system

By means of the Newman product combination, the source function of the finite-length strip with center (x_w, y_w) , width y_f and length x_f is obtained as:

$$S(x, y, t) = \frac{1}{4} \left[\text{erf} \frac{\frac{x_f}{2} + (x - x_w)}{\sqrt{4\eta t}} + \text{erf} \frac{\frac{x_f}{2} - (x - x_w)}{\sqrt{4\eta t}} \right] \cdot \left[\text{erf} \frac{\frac{y_f}{2} + (y - y_w)}{\sqrt{4\eta t}} + \text{erf} \frac{\frac{y_f}{2} - (y - y_w)}{\sqrt{4\eta t}} \right] \quad (7)$$

Considering the development of natural fractures in the reservoir, the flow equation of natural fracture system is:

$$\frac{\partial^2 p_f}{\partial x^2} + \frac{\partial^2 p_f}{\partial y^2} + \frac{\alpha_m k_m}{k_f} (p_m - p_f) + 2\pi\delta(x - x_w)\delta(y - y_w) = \frac{\mu\phi_f c_{if}}{k_f} \frac{\partial p_f}{\partial t} \quad (8)$$

Differential equations for flow in matrix systems:

$$\frac{\partial(\rho\phi_m)}{\partial t} + q_{ex} = 0 \quad (9)$$

$$q_{ex} = \frac{\alpha_m k_m \rho}{\mu} (p_m - p_f) \quad (10)$$

Initial condition:

$$p_f(x, y, 0) = p_m(x, y, 0) = p_i \quad (11)$$

Boundary condition:

Along the x-coordinate

$$\frac{\partial p_f(0, y, t)}{\partial x} = 0, \quad \frac{\partial p_f(x_e, y, t)}{\partial x} = 0 \quad (12)$$

Along the y-coordinate

$$\frac{\partial p_f(x, 0, t)}{\partial y} = 0, \quad \frac{\partial p_f(x, y_e, t)}{\partial y} = 0 \quad (13)$$

If the transient flow rate of this finite-length strip source function is dl , then the pressure drop induced by this transient source at point M is:

$$\Delta p(M, t) = \frac{dl}{4x_f y_f \phi c} \left[\operatorname{erf} \frac{\frac{x_f}{2} + (x - x_w)}{\sqrt{4\eta_f t}} + \operatorname{erf} \frac{\frac{x_f}{2} - (x - x_w)}{\sqrt{4\eta_f t}} \right] \left[\operatorname{erf} \frac{\frac{y_f}{2} + (y - y_w)}{\sqrt{4\eta_f t}} + \operatorname{erf} \frac{\frac{y_f}{2} - (y - y_w)}{\sqrt{4\eta_f t}} \right] \quad (14)$$

As the pressure drop in the formation brought on by a single volume fracturing section, the pressure fluctuations brought on by a finite-length transient strip source function with a given flow rate at a specific position can be described. In order to mimic the pressure field characteristics under synergistic flow with multiple fracture segments, it is necessary to superimpose several finite-length strip sources in the plane in general volume fracturing horizontal wells with multiple fracture modification strips.

The model is mathematically described as having Q production flow rate and N finite-length fracture strips. For the point at coordinates (x, y) , the pressure decrease that is caused at time t is

$$\Delta p(x, y, t) = \sum_{k=1}^N \frac{Q \cdot B}{4hx_f y_f \phi c} \cdot \left[\operatorname{erf} \frac{\frac{x_f}{2} + (x - x_k)}{\sqrt{4\eta_f t}} + \operatorname{erf} \frac{\frac{x_f}{2} - (x - x_k)}{\sqrt{4\eta_f t}} \right] \left[\operatorname{erf} \frac{\frac{y_f}{2} + (y - y_k)}{\sqrt{4\eta_f t}} + \operatorname{erf} \frac{\frac{y_f}{2} - (y - y_k)}{\sqrt{4\eta_f t}} \right] \quad (15)$$

Then the actual pressure distribution in the formation is:

$$p(x, y, t) = p_e - \Delta p(x, y, t) \quad (16)$$

The principle of superposition of unsteady flow must be applied to create a model of volume fractured horizontal wells under the condition of variable production in the matrix region and the SRV region, where the permeability of the SRV is much greater than that of the matrix region, if it is necessary to take into account the unsteady flow under the condition of fixed bottomhole flow pressure and the condition of nonlinear flow.

The pressure drop caused by the k th fracture strip with historical flow rate Q_k to the location with coordinates (x, y) at moment t is as follows, taking into account unsteady flow and nonlinear flow conditions:

$$\Delta p(x, y, t) = \frac{B}{4hx_f y_f \phi c} \sum_{k=1}^N \sum_{i=1}^n (Q_{k,i} - Q_{k,i-1}) \int_0^{t_n - t_{i-1}} \left[\operatorname{erf} \frac{\frac{x_f}{2} + (x - x_k)}{\sqrt{4\eta_f t}} + \operatorname{erf} \frac{\frac{x_f}{2} - (x - x_k)}{\sqrt{4\eta_f t}} \right] \left[\operatorname{erf} \frac{\frac{y_f}{2} + (y - y_k)}{\sqrt{4\eta_f t}} + \operatorname{erf} \frac{\frac{y_f}{2} - (y - y_k)}{\sqrt{4\eta_f t}} \right] dt \quad (17)$$

The formation pressure distribution is:

$$p(x, y, t) = p_e - \frac{B}{4hx_f y_f \phi c} \sum_{k=1}^N \sum_{i=1}^n (Q_{k,i} - Q_{k,i-1}) \int_0^{t_n - t_{i-1}} \left[\operatorname{erf} \frac{\frac{x_f}{2} + (x - x_k)}{\sqrt{4\eta_f t}} + \operatorname{erf} \frac{\frac{x_f}{2} - (x - x_k)}{\sqrt{4\eta_f t}} \right] \left[\operatorname{erf} \frac{\frac{y_f}{2} + (y - y_k)}{\sqrt{4\eta_f t}} + \operatorname{erf} \frac{\frac{y_f}{2} - (y - y_k)}{\sqrt{4\eta_f t}} \right] dt \quad (18)$$

The formation pressure gradient distribution is:

$$\frac{\partial p}{\partial x} = -\frac{1}{4\sqrt{\pi\eta_t}} \cdot \frac{B}{hx_f y_f \phi c} \cdot \sum_{k=1}^N \sum_{i=1}^n (Q_{k,i} - Q_{k,i-1}) \int_0^{t_n-t_{i-1}} \left\{ \exp \left[-\frac{\left(\frac{x_f}{2} + (x-x_k) \right)^2}{4\eta_t t} \right] - \exp \left[-\frac{\left(\frac{x_f}{2} - (x-x_k) \right)^2}{4\eta_t t} \right] \right\} \left[\operatorname{erf} \frac{\frac{y_f}{2} + (y-y_k)}{\sqrt{4\eta_t t}} + \operatorname{erf} \frac{\frac{y_f}{2} - (y-y_k)}{\sqrt{4\eta_t t}} \right] dt \quad (19)$$

$$\frac{\partial p}{\partial y} = -\frac{1}{4\sqrt{\pi\eta_t}} \cdot \frac{B}{hx_f y_f \phi c} \cdot \sum_{k=1}^N \sum_{i=1}^n (Q_{k,i} - Q_{k,i-1}) \int_0^{t_n-t_{i-1}} \left[\operatorname{erf} \frac{\frac{x_f}{2} + (x-x_k)}{\sqrt{4\eta_t t}} + \operatorname{erf} \frac{\frac{x_f}{2} - (x-x_k)}{\sqrt{4\eta_t t}} \right] \left\{ \exp \left[-\frac{\left(\frac{y_f}{2} + (y-y_k) \right)^2}{4\eta_t t} \right] - \exp \left[-\frac{\left(\frac{y_f}{2} - (y-y_k) \right)^2}{4\eta_t t} \right] \right\} dt \quad (20)$$

Using linear flow conditions, the mathematical model above depicts unsteady flow in volumetrically broken horizontal wells at a specific instant. The permeability is functionally connected to the pressure gradient by linearizing the nonlinear flow equation, and the above model characterizes the nonlinear flow process through the time-varying permeability.

3.3 Solution Methodology

3.3.1 Treatment of nonlinear flow in transient pressure modeling

Every transient moment's pressure distribution and pressure gradient distribution (Eq (12), (13), and (14)), in which the pressure conductivity coefficients are the magnitudes of the fluctuations correlated with the pressure gradient, exhibit nonlinear permeability. The following equation can be used to determine the pressure conductivity at various times:

$$\eta_{(t)} = \frac{K_{e(t_{i-1})}}{\phi C_i} \quad (21)$$

$$K_{e(t)} = \frac{\sum_{r=0.1}^{Rt} \frac{K_{e(t_{i-1})}}{\mu} \cdot \left(1 - \frac{1}{a + b \nabla p_{r(t_{i-1})}} \right)}{Rt}$$

Solving the pressure function of the model requires that the flow Q be solved individually for each discrete instant moment. The solution procedure for the flow rate $Q_{k,n}$ for the K th fracture strip at time t is as follows:

$$\Delta p(x, y, x_k, y_k, t) = A(x, y, x_k, y_k, t) Q_{k,n} + B(x, y, x_k, y_k, t) \quad (22)$$

Among which:

$$A(x, y, x_k, y_k, t) = \frac{B}{4hx_f y_f \phi c} \int_0^{t_n-t_{i-1}} \left[\operatorname{erf} \frac{\frac{x_f}{2} + (x-x_k)}{\sqrt{4\eta_t t}} + \operatorname{erf} \frac{\frac{x_f}{2} - (x-x_k)}{\sqrt{4\eta_t t}} \right] \left[\operatorname{erf} \frac{\frac{y_f}{2} + (y-y_k)}{\sqrt{4\eta_t t}} + \operatorname{erf} \frac{\frac{y_f}{2} - (y-y_k)}{\sqrt{4\eta_t t}} \right] dt \quad (23)$$

$$B(x, y, x_k, y_k, t) = -\frac{Q_{k,n} B}{4hx_f y_f \phi c} \int_0^{t_n-t_{i-1}} \left[\operatorname{erf} \frac{\frac{x_f}{2} + (x-x_k)}{\sqrt{4\eta_t t}} + \operatorname{erf} \frac{\frac{x_f}{2} - (x-x_k)}{\sqrt{4\eta_t t}} \right] \left[\operatorname{erf} \frac{\frac{y_f}{2} + (y-y_k)}{\sqrt{4\eta_t t}} + \operatorname{erf} \frac{\frac{y_f}{2} - (y-y_k)}{\sqrt{4\eta_t t}} \right] dt + \frac{B}{4hx_f y_f \phi c} \sum_{i=1}^{n-1} (Q_{k,i} - Q_{k,i-1}) \int_0^{t_n-t_{i-1}} \left[\operatorname{erf} \frac{\frac{x_f}{2} + (x-x_k)}{\sqrt{4\eta_t t}} + \operatorname{erf} \frac{\frac{x_f}{2} - (x-x_k)}{\sqrt{4\eta_t t}} \right] \left[\operatorname{erf} \frac{\frac{y_f}{2} + (y-y_k)}{\sqrt{4\eta_t t}} + \operatorname{erf} \frac{\frac{y_f}{2} - (y-y_k)}{\sqrt{4\eta_t t}} \right] dt \quad (24)$$

Under the condition that $\Delta p(x, y, x_k, y_k, t)$ is known, it can be found that for the k th fracture strip flow rate $Q_{k,n}$, $\Delta p(x, y, x_k, y_k, t)$ at the k th fracture strip of the volume fractured horizontal wells is jointly acted on by N fractures, then we have:

$$\Delta p(x, y, t) = \sum_{k=1}^N \Delta p(x, y, x_k, y_k, t) \quad (25)$$

The flow solution equation can be constructed for Eq.(19) as follows:

$$\Delta p(x, y, t) = \sum_{k=1}^N A(x, y, x_k, y_k, t) Q_{k,n} + B(x, y, x_k, y_k, t) \quad (26)$$

At a specific production differential pressure, $\Delta p = p_e - p_{wf}$ is a known quantity, and a flow matrix for solving multiple fracturing strips is established:

$$\begin{bmatrix} A(x_1, y_1, x_1, y_1, t) & \cdots & A(x_1, y_1, x_N, y_N, t) \\ \vdots & \ddots & \vdots \\ A(x_N, y_N, x_1, y_1, t) & \cdots & A(x_N, y_N, x_N, y_N, t) \end{bmatrix} \begin{bmatrix} Q_{1,n} \\ \vdots \\ Q_{N,n} \end{bmatrix} + \begin{bmatrix} \sum_{k=1}^N B(x_1, y_1, x_k, y_k, t) \\ \vdots \\ \sum_{k=1}^N B(x_N, y_N, x_k, y_k, t) \end{bmatrix} = \begin{bmatrix} \Delta p \\ \vdots \\ \Delta p \end{bmatrix} \quad (27)$$

After obtaining the $Q_{k,n}$ of various fracturing strips at time t , the apparent permeability K_e as well as the conductivity coefficient η_t are solved. The pressure distribution formula and pressure gradient distribution formula (Eq.(12),(13),(14)) are then brought back to obtain the formation pressure distribution and pressure gradient distribution.

The location of the pressure propagation dynamic boundary of volume fractured horizontal wells is

identified as follows for the nonlinear flow circumstances at various moments:

$$\begin{aligned} \left(\frac{\partial p}{\partial x} - G_a \right) \Big|_{r=Rtx} &= 0 \\ \left(\frac{\partial p}{\partial y} - G_a \right) \Big|_{r=Rty} &= 0 \\ G_a &= \frac{1-a}{b} \end{aligned} \quad (28)$$

According to the nonlinear flow treatment, the pressure propagation dynamic boundary is where the formation pressure gradient equals the critical initiation pressure gradient. With an apparent permeability of 0 outside of this area, the formation keeps its initial formation pressure.

3.3.2 Pressure propagation dynamic boundary solution

The iterative solution procedure for the pressure propagation dynamic boundary of volume fractured horizontal wells considering nonlinear flow is as follows:

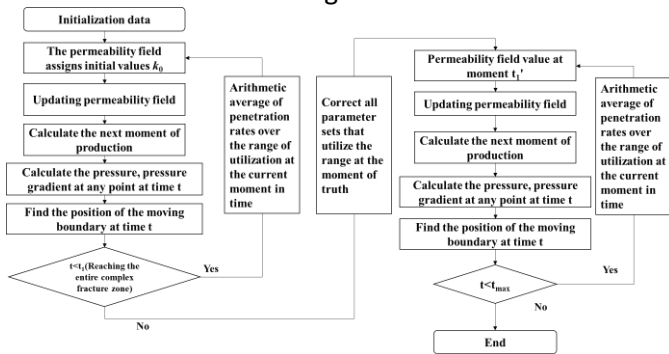


Fig. 3 Dynamic boundary solution process of pressure propagation

3.3.3 Numerical solution and iteration of apparent permeability

To generate a curve for the fluctuation of apparent permeability with pressure gradient, an expression for the relationship between apparent permeability and pressure gradient was established. Nonlinear flow in shale reservoirs was studied using a two-parameter continuous flow model:

$$v = -\frac{K}{\mu} \cdot \nabla p \left(1 - \frac{1}{a + b \nabla p} \right) \quad (29)$$

Define the expression for apparent permeability versus pressure gradient as:

$$K_e = K_i \left(1 - \frac{1}{a + b \nabla p} \right) \quad (30)$$

The differentiation principle is used to linearize the flow curve into segments. Any part of a pressure gradient

is viewed as linear flow, and each linear section's apparent permeability is related to the pressure gradient, which is a constant if the pressure gradient changes very little. In accordance with each extremely brief pressure gradient section, there:

$$v = -\frac{K_e(\nabla p)}{\mu} \cdot \nabla p = -\left[\frac{K_0 \left(1 - \frac{1}{a + b \nabla p} \right)}{\mu} \right] \cdot \nabla p \quad (31)$$

A linear differential equation is created from a line of nonlinear percolation differential equations. The nonlinear flow process refers to the superposition of linear flow at discrete multiple transient periods for a particular production duration.

① The initial value of permeability is initially allocated, and for the moment t_n , given the initial value of permeability, see Eq (21), it is discovered that Q is the flow rate of the various fracturing segments at the moment. After that, begin to iteratively solve the formation pressure distribution and formation pressure gradient distribution until the formation pressure gradient between two sites is less than or equal to the startup pressure gradient, at which time the iteration finishes, and the subsequent iterative computation begins. The formation is in an inactive condition during the first production moment, and the original formation permeability serves as the beginning value of the flow rate.

② The permeability values at various locations under each moment are determined using the distribution of the formation pressure gradient under each moment and the relationship between apparent permeability and pressure gradient. The permeability values within the pressure propagation distance at the moment are then geometrically averaged, see Equation (15), and this value is used as the initial permeability at the following moment.

③ To determine the pressure propagation boundaries for various production durations, repeat steps 1 and 2 in their entirety.

4. MATERIAL AND METHODS

The pressure field waves and characteristics of the near-well zone during the production of a single well are depicted based on the decay development method of the actual fixed bottomhole flow pressure in the mine site, and the effects of natural fractures, geological parameters, etc., on the pressure waves and the movement of the dynamic boundary are analyzed.

4.1 Effect of natural fractures on moving boundaries

In volume fractured horizontal wells, the mobilization distance in various directions is significantly increased by the existence of natural fractures, and the inflection point is the location of an abrupt change in permeability, which shows that the pressure wave has reached the matrix region; Accordingly, the moving boundary movement distance in the perpendicular to the wellbore direction is greater than that along the wellbore direction, and the range of early movement in the perpendicular to the wellbore direction is greater. This is because the perpendicular to the wellbore direction is the extension direction of the fractured fracture, which is the main direction of fluid flow.

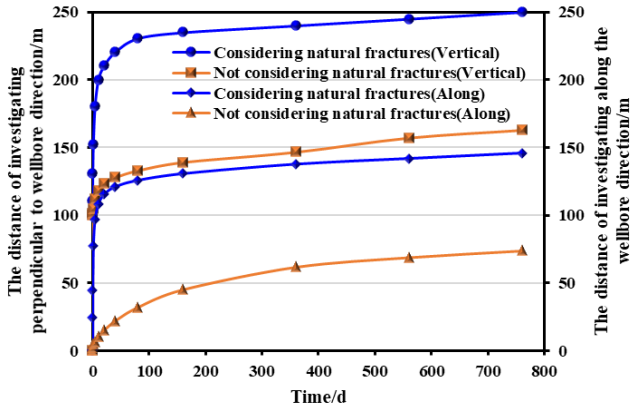


Fig. 4 Plot of the effect of natural fractures on dynamic boundary of pressure propagation

4.2 Effect of reservoir initial permeability on moving boundary

Figure 5 depicts the pressure propagation dynamic boundaries for various permeability conditions as a function of time in the perpendicular to wellbore direction. For various permeability conditions, Figure 6 depicts the pressure propagation dynamic boundaries along the wellbore direction as a function of time. Similar movement patterns can be seen in the moving boundaries of volume fractured horizontal wells in all directions. In the early stages of production, the dynamic boundaries spread out more quickly and their distance from each other increases, but as production goes on, this distance tends to stabilize and stop changing.

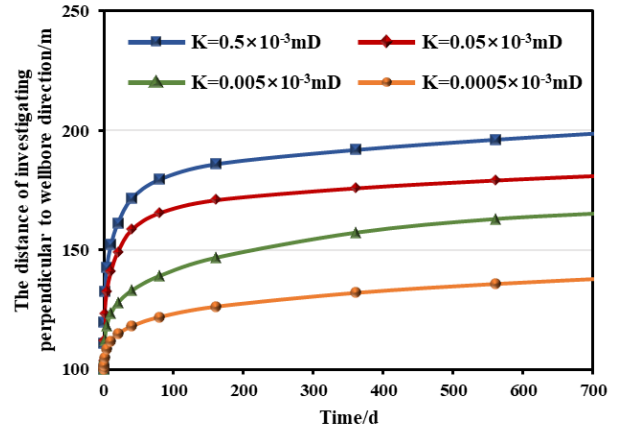


Fig. 5 Dynamic boundary move distance over time (perpendicular to wellbore direction)

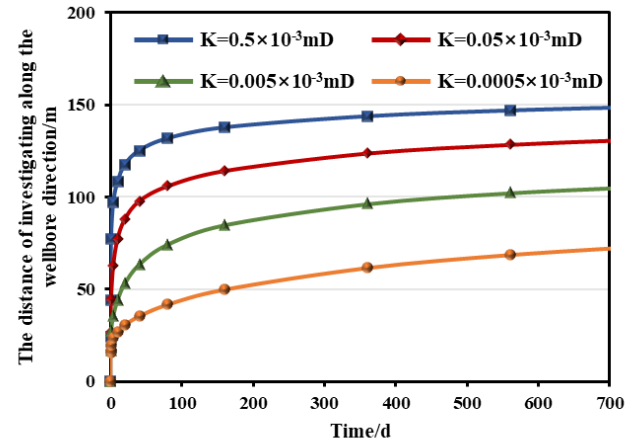


Fig. 6 Dynamic boundary move distance over time (along the wellbore direction)

4.3 The effects of dynamic boundary in different directions

In volume fractured horizontal wells, the dynamic boundary's moving distance in various directions exhibits a rapid increase in the early stages and a steady pattern in the later stages. The dynamic boundary's movement rate exhibits a "L" pattern. In addition, the rate of dynamic boundary movement slows down more gradually in the wellbore direction. Therefore, while planning well spacing in horizontal wells for fracturing shale reservoirs, this aspect should be taken into consideration.

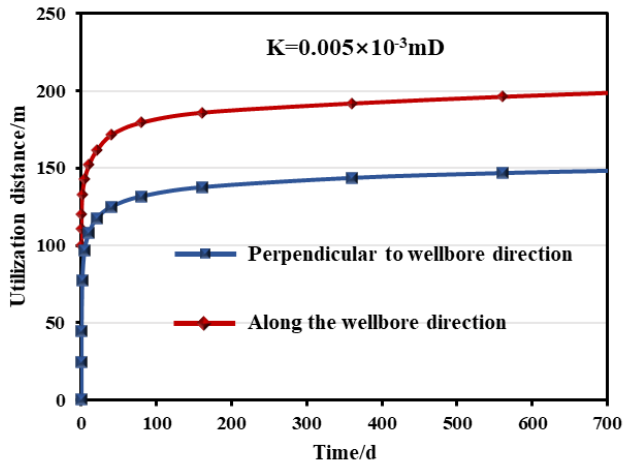


Fig. 7 Comparison of dynamic boundary moving distance in different directions

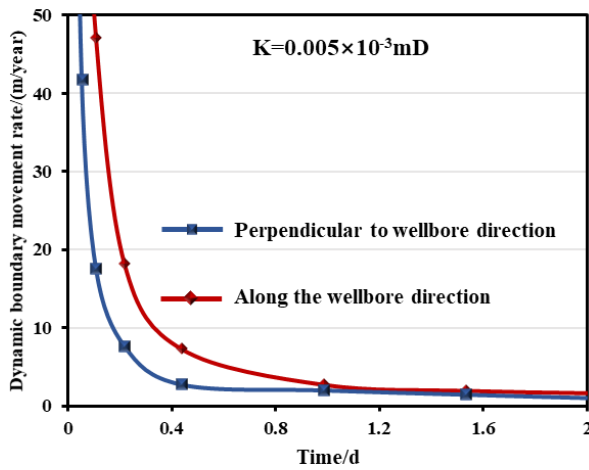


Fig. 8 Comparison of dynamic boundary movement rates in different directions

5. CONCLUSIONS

(1) A novel unsteady porous flow model of volume fractured horizontal wells with developed natural fractures is established to characterize the pressure propagation and mobilization distance of shale oil reservoir with developed natural fractures.

(2) The mobilization distance of volume fractured horizontal wells can be significantly increased by the existence of natural fractures. The direction perpendicular to the wellbore is the direction of extension of hydraulic fractures, that is, the direction of the main streamline. Hence, the distance propagated by the dynamic boundary perpendicular to the wellbore direction is longer than the distance propagated along the wellbore direction.

(3) The movement rate of dynamic boundary displays a decreasing "L" pattern. In the early period, dynamic boundary movement rates are increasing

quickly due to the abundance of both natural fractures and hydraulic fractures in the SRV region. However, the movement rate of dynamic boundary is steady when the pressure is propagated to the matrix region.

ACKNOWLEDGEMENT

The authors acknowledge that this study was partially supported by the National Natural Science Foundation of China (No. 52174038 and No. 52004307), China Petroleum Science and Technology Project-major project-Research on tight oil-shale oil reservoir engineering methods and key technologies in Ordos Basin (ZLZX2020-02-04) and Science Foundation of China University of Petroleum, Beijing (No. 2462018YJRC015).

DECLARATION OF INTEREST STATEMENT

The authors declare that they have no known competing financial interests or personal relationships that could have appeared to influence the work reported in this paper. All authors read and approved the final manuscript.

REFERENCE

- [1] Alnoaimi, Khalid R., Christophe Duchateau, and Anthony R. Kovscek. "Characterization and measurement of multiscale gas transport in shale-core samples." *SPE Journal* 21.02 (2016): 573-588.
- [2] Duda, J. R., et al. "Hydraulic Fracturing: The Forgotten Key to Natural Gas Supply." *SPE Unconventional Resources Conference/Gas Technology Symposium*. SPE, 2002.
- [3] Muskat M. *The flow of homogeneous fluids through porous media*[M]. New York: McGrawhill, 1937:9-150.
- [4] Prada A, Civan F. Modification of Darcy's law for the threshold pressure gradient[J]. *Journal of Petroleum Science and Engineering*, 1999, 22(4): 237-240.
- [5] Rong-Ze Y, Qun L, Zheng-Ming Y, et al. Nonlinear flow numerical simulation of an ultra-low permeability reservoir[J]. *Chinese Physics Letters*, 2010, 27(7): 074702.
- [6] Xu, Jianchun, et al. "Non-Darcy flow numerical simulation for low-permeability reservoirs." *SPE Europe conference and exhibition*. SPE, 2012.
- [7] Bezyan, Yashar, et al. "A novel approach for solving nonlinear flow equations: The next step towards an accurate assessment of shale gas resources." *Fuel* 236 (2019): 622-635.
- [8] Jia, Zhihao, et al. "Full composition numerical simulation of CO₂ utilization process in shale reservoir using projection-based embedded discrete fracture

model (pEDFM) considering nano-confinement effect." Gas Science and Engineering 111 (2023): 204932.

[9] Cao, Renyi, et al. "Using high-intensity water flooding relative permeability curve for predicting mature oilfield performance after long-term water flooding in order to realize sustainable development." Journal of Petroleum Science and Engineering 215 (2022): 110629.

[10] Wang, L., Yang, SH. L. & Meng, ZH. et al. Time-dependent shape factors for fractured reservoir simulation: Effect of stress sensitivity in matrix system[J].Journal of Petroleum Science and Engineering, 2018, 163: 556-569.

[11] Liu W, Zhang Q, Dong Y, et al. Analytical and numerical studies on a moving boundary problem of non-Newtonian Bingham fluid flow in fractal porous media[J]. Physics of Fluids, 2022, 34(2): 023101.